Plane-Line-Shadow SLAM

Sun Qinxuan

June 3, 2019

OUTLINE

Problem Formulation

- Plane-line-based map
  - Plane features: $\{\boldsymbol{\pi}_j\}_{j=1,\cdots,N_\pi}$.
  - Line features: $\{\boldsymbol{\mathcal{L}}_k\}_{k=1,\cdots,N_\mathcal{L}}$.

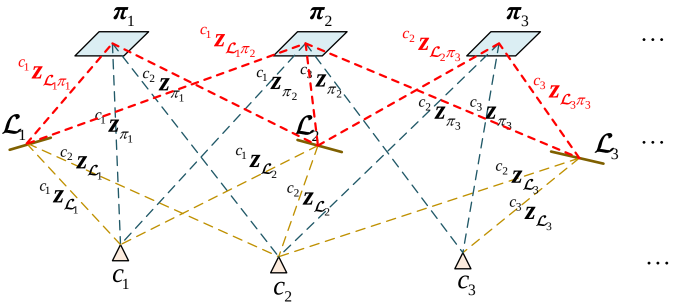

Problem Formulation

- Observations
  - ${}^{c_i}\boldsymbol{z}_{\pi_j} = [{}^{c_i}\boldsymbol{n}_{\pi_j}^T, {}^{c_i}d_{\pi_j}]^T$ – observation of the j-th plane in i-th camera frame.
  - ${}^{c_i}\boldsymbol{z}_{\mathcal{L}_k} = [{}^{c_i}\tilde{\boldsymbol{u}}_{\mathcal{L}_k}^T, {}^{c_i}\tilde{\boldsymbol{v}}_{\mathcal{L}_k}^T]^T$ – observation of the k-th line in i-th camera frame.
  - ${}^{c_i}\boldsymbol{z}_{\mathcal{L}_k\pi_j} = [{}^{c_i}\tilde{\boldsymbol{u}}_{\mathcal{L}_k\pi_j}^T, {}^{c_i}\tilde{\boldsymbol{v}}_{\mathcal{L}_k\pi_j}^T]^T$ – projections of the observation of the k-th line onto the observation of the j-th plane in i-th camera frame.

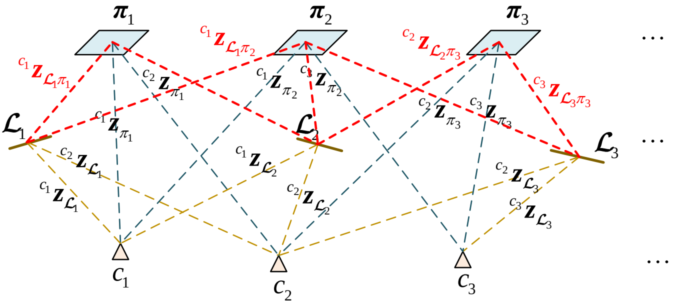

Problem Formulation

- Problem Formulation
  - Given the observations ${}^{c_i}\boldsymbol{z}_{\pi_j}$, ${}^{c_i}\boldsymbol{z}_{\mathcal{L}_k}$ and ${}^{c_i}\boldsymbol{z}_{\mathcal{L}_k\pi_j}$, find the optimal camera poses $\{\boldsymbol{R}_{c_ig},\boldsymbol{t}_{c_ig}\}_{i=1,\cdots,N_c}$ planes $\{\boldsymbol{\pi}_j\}_{j=1,\cdots,N_\pi}$ and lines $\{\boldsymbol{\mathcal{L}}_k\}_{k=1,\cdots,N_\mathcal{L}}$ such that (1) is minimized.

$$\begin{aligned}&\sum_{i=1}^{N_c}\sum_{j=1}^{N_\pi}{}^{c_i}\boldsymbol{e}_{\pi_j}^T\,{}^{c_i}\boldsymbol{\Omega}_{\pi_j}\,{}^{c_i}\boldsymbol{e}_{\pi_j}+\sum_{i=1}^{N_c}\sum_{k=1}^{N_\mathcal{L}}{}^{c_i}\boldsymbol{e}_{\mathcal{L}_k}^T\,{}^{c_i}\boldsymbol{\Omega}_{\mathcal{L}_k}\,{}^{c_i}\boldsymbol{e}_{\mathcal{L}_k}\\&+\sum_{i=1}^{N_c}\sum_{j=1}^{N_\pi}\sum_{k=1}^{N_\mathcal{L}}\alpha(i,j,k)\,{}^{c_i}\boldsymbol{e}_{\mathcal{L}_k\pi_j}^T\,{}^{c_i}\boldsymbol{\Omega}_{\mathcal{L}_k\pi_j}\,{}^{c_i}\boldsymbol{e}_{\mathcal{L}_k\pi_j}\end{aligned}\tag{1}$$

  with

$$\begin{aligned}{}^{c_i}\boldsymbol{e}_{\pi_j}&={}^{c_i}\boldsymbol{z}_{\pi_j}-\varphi_\pi(\boldsymbol{R}_{c_ig},\boldsymbol{t}_{c_ig},\boldsymbol{\pi}_j)\\{}^{c_i}\boldsymbol{e}_{\mathcal{L}_k}&={}^{c_i}\boldsymbol{z}_{\mathcal{L}_k}-\varphi_\mathcal{L}(\boldsymbol{R}_{c_ig},\boldsymbol{t}_{c_ig},\boldsymbol{\mathcal{L}}_k)\\{}^{c_i}\boldsymbol{e}_{\mathcal{L}_k\pi_j}&={}^{c_i}\boldsymbol{z}_{\mathcal{L}_k\pi_j}-\varphi_{\mathcal{L}\pi}(\boldsymbol{R}_{c_ig},\boldsymbol{t}_{c_ig},\boldsymbol{\mathcal{L}}_k,\boldsymbol{\pi}_j)\end{aligned}\tag{2}$$

  - $\alpha(i,j,k)=1$ if $\boldsymbol{\mathcal{L}}_k$ and $\boldsymbol{\pi}_j$ are both observed in camera i. Otherwise, $\alpha(i,j,k)=0$.

Problem Formulation

- Problem Formulation
  - $\varphi_{\pi}(\boldsymbol{R}_{c_i g}, \boldsymbol{t}_{c_i g}, \boldsymbol{\pi}_j)$ and $\varphi_{\mathcal{L}}(\boldsymbol{R}_{c_i g}, \boldsymbol{t}_{c_i g}, \boldsymbol{\mathcal{L}}_k)$ are plane and line observation models, respectively (introduced in Section 1.1).
  - ${}^{c_i}\boldsymbol{\Omega}_{\pi_j}$ and ${}^{c_i}\boldsymbol{\Omega}_{\mathcal{L}_k}$ are the information matrices for planes and lines, respectively (introduced in Section 4).
  - $\varphi_{\mathcal{L}\pi}(\boldsymbol{R}_{c_i g}, \boldsymbol{t}_{c_i g}, \boldsymbol{\mathcal{L}}_k, \boldsymbol{\pi}_j)$ is the shadow observation model (introduced in Section 1.2).
  - ${}^{c_i}\boldsymbol{\Omega}_{\mathcal{L}_k \pi_j}$ is the information matrices for line shadows (introduced in Section 1.2).

Parameterization for Planes

- A plane equation in 3-space $\Pi_1 X + \Pi_2 Y + \Pi_3 Z + \Pi_4 = 0$ is unaffected by multiplication by a non-zero scalar – a plane has 3 degrees of freedom in 3-space.
- The homogeneous representation of the plane is $\mathbf{\Pi} = [\Pi_1, \Pi_2, \Pi_3, \Pi_4]^T \in \mathbb{P}^3$ in projective space. [1]
- Spherically normalizing the homogeneous vector $\mathbf{\Pi}$ yields $\boldsymbol{\pi} = \mathbf{\Pi} / \|\mathbf{\Pi}\| \in \mathbb{S}^3$.
- $\mathbb{S}^3$ is the 3-sphere in the space $\mathbb{R}^4$, which is a Lie group under the operation of quaternion multiplication when its elements are viewed as unit quaternions.

[1] R. Hartley and A. Zisserman, "Multiple View Geometry in Computer Vision". Cambridge University Press, 2003, second Edition.

Minimal Parameterization for Planes

- Since there are four directions in which $\boldsymbol{\pi}$ can change in an optimization process, but the plane only has three DOFs. An optimizer is free to move the variable off the unit quaternion sphere.
- We use the exponential map from $\mathbb{R}^3$ to $\mathbb{S}^3$: [2] [3]

$$\exp(\boldsymbol{\zeta}) = \begin{cases} \left[\frac{1}{\|\boldsymbol{\zeta}\|}\sin(\frac{1}{2}\|\boldsymbol{\zeta}\|)\hat{\boldsymbol{\zeta}}, \sin(\frac{1}{2}\|\boldsymbol{\zeta}\|)\right]^T & \textit{if} \quad \boldsymbol{\zeta} \neq 0 \\ [0,0,0,1]^T & \textit{if} \quad \boldsymbol{\zeta} = 0 \end{cases} \tag{3}$$

with $\boldsymbol{\zeta} \in \mathbb{R}^3$ and $\hat{\boldsymbol{\zeta}} = \boldsymbol{\zeta}/\|\boldsymbol{\zeta}\|$.

- A plane $\boldsymbol{\pi} \in \mathbb{S}^3$ is updated by an increment $\boldsymbol{\zeta} \in \mathbb{R}^3$ using the quaternion multiplication

$$\boldsymbol{\pi}' = \exp(\boldsymbol{\zeta}) \circ \boldsymbol{\pi} \tag{4}$$

[2] M. Kaess, “Simultaneous localization and mapping with infinite planes”, 2015 IEEE International Conference on Robotics and Automation (ICRA), 2015, pp. 4605-4611.

[3] Grassia, and F. Sebastian . “Practical Parameterization of Rotations Using the Exponential Map”. Journal of Graphics Tools 3.3(1998): 29-48.

Observation Model

- Plane observation model

$$\varphi_\pi(\boldsymbol{R}_{cg}, \boldsymbol{t}_{cg}, \boldsymbol{\pi}) = \begin{bmatrix} \boldsymbol{R}_{cg} & 0 \\ -\boldsymbol{t}_{cg}^T \boldsymbol{R}_{cg} & 1 \end{bmatrix} \cdot \begin{bmatrix} \boldsymbol{n} \\ d \end{bmatrix} \tag{5}$$

  with

$$\begin{bmatrix} \boldsymbol{n} \\ d \end{bmatrix} = \frac{\boldsymbol{\pi}}{\pi_1^2 + \pi_2^2 + \pi_3^2} \tag{6}$$

  and $\boldsymbol{\pi} = [\pi_1, \pi_2, \pi_3, \pi_4]^T$.
- ${}^c\boldsymbol{n}$ and ${}^c d$ are the unit normal of the plane and the vertical distance from the origin to the plane, respectively, expressed in the camera coordinate frame.
- $\boldsymbol{R}_{cg} \in \mathbb{SO}(3)$ and $\boldsymbol{t}_{cg} \in \mathbb{R}^3$ are the rotation matrix and the translation vector from the global coordinate frame to the camera coordinate frame, respectively.

Plücker Coordinates of 3D Lines

- The Plücker coordinates of a 3D line are denoted by $\boldsymbol{\mathcal{L}} = [\boldsymbol{u}^T, \boldsymbol{v}^T]^T \in \mathbb{P}^5$ and satisfy the Plücker constraint $\boldsymbol{u}^T \boldsymbol{v} = 0$.
- $\boldsymbol{u} \in \mathbb{R}^3$ is normal to the interpretation plane $\boldsymbol{\pi}_{\mathcal{L}}$ containing the line $\boldsymbol{\mathcal{L}}$.
- $\boldsymbol{v} \in \mathbb{R}^3$ is the line direction.
- The vertical distance from the origin to the line is computed by $\|\boldsymbol{u}\| / \|\boldsymbol{v}\|$.

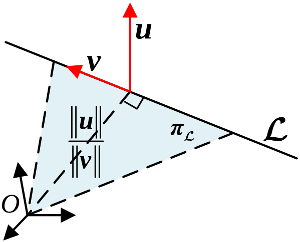

Orthonormal Representation for 3D Lines

- The orthonormal representation [4] enables the local update of the Plücker coordinates using the minimum number of parameters.
- Any (projective) 3D line can be represented by [5]

$$(\boldsymbol{Q}, \boldsymbol{W}) \in \mathbb{SO}(3) \times \mathbb{SO}(2) \tag{7}$$

$(\boldsymbol{Q}, \boldsymbol{W})$ is the orthonomal representation of a 3D line.

[4] Bartoli, Adrien . "On the Non-Linear Optimization of Projective Motion Using Minimal Parameters". 7th European Conference on Computer Vision Springer-Verlag, 2002.

[5] Bartoli, Adrien , and P. Sturm . "Structure-from-motion using lines: Representation, triangulation, and bundle adjustment". Computer Vision and Image Understanding 100.3(2005):416-441.

Relating Plücker coordinates and orthonormal representation [6]

- The 3×2 matrix $[\boldsymbol{u}|\boldsymbol{v}]$ can be factored as

$$[\boldsymbol{u}|\boldsymbol{v}] = \boldsymbol{Q}\boldsymbol{\Sigma} \tag{8}$$

with

$$\begin{aligned} \boldsymbol{Q} &= \begin{bmatrix} \frac{\boldsymbol{u}}{\|\boldsymbol{u}\|} & \frac{\boldsymbol{v}}{\|\boldsymbol{v}\|} & \frac{\boldsymbol{u}\times\boldsymbol{v}}{\|\boldsymbol{u}\times\boldsymbol{v}\|} \end{bmatrix} \in \mathbb{SO}(3) \\ \boldsymbol{\Sigma} &= \begin{bmatrix} \|\boldsymbol{u}\| & 0 \\ 0 & \|\boldsymbol{v}\| \\ 0 & 0 \end{bmatrix} \end{aligned} \tag{9}$$

[6] Bartoli, Adrien , and P. Sturm . "Structure-from-motion using lines: Representation, triangulation, and bundle adjustment". Computer Vision and Image Understanding 100.3(2005):416-441.

Relating Plücker coordinates and orthonormal representation [7]

- Set

$$\boldsymbol{W} = \begin{bmatrix} \sigma_1 & -\sigma_2 \\ \sigma_2 & \sigma_1 \end{bmatrix} \in \mathbb{SO}(2) \tag{10}$$

with

$$\begin{aligned} \sigma_1 &= \frac{\|\boldsymbol{u}\|}{\sqrt{\|\boldsymbol{u}\|^2 + \|\boldsymbol{v}\|^2}} \\ \sigma_2 &= \frac{\|\boldsymbol{v}\|}{\sqrt{\|\boldsymbol{u}\|^2 + \|\boldsymbol{v}\|^2}} \end{aligned} \tag{11}$$

[7] Bartoli, Adrien , and P. Sturm . "Structure-from-motion using lines: Representation, triangulation, and bundle adjustment". Computer Vision and Image Understanding 100.3(2005):416-441.

Relating Plücker coordinates and orthonormal representation [8]

- The minimum four line parameters are denoted by $\boldsymbol{\eta} = [\boldsymbol{\theta}^T, \theta]^T$ where $\boldsymbol{\theta} \in \mathbb{R}^3$ and $\theta \in \mathbb{R}$.
- $\boldsymbol{Q}$ and $\boldsymbol{W}$ are updated by

$$\begin{aligned} \boldsymbol{Q} &= \boldsymbol{Q} \exp([\boldsymbol{\theta}]_\times) \\ \boldsymbol{W} &= \boldsymbol{W} \exp([\theta]_\times) \end{aligned} \tag{12}$$

where $[\boldsymbol{\theta}]_\times$ and $[\theta]_\times$ are the 3×3 and 2×2 skew symmetric matrices corresponding to $\boldsymbol{\theta}$ and θ, respectively.

[8] Bartoli, Adrien , and P. Sturm . "Structure-from-motion using lines: Representation, triangulation, and bundle adjustment". Computer Vision and Image Understanding 100.3(2005):416-441.

Relating Plücker coordinates and orthonormal representation [9]

- Converting from the orthnormal representation $(\boldsymbol{Q}, \boldsymbol{W})$ to the Plücker coordinates $\mathcal{L}$ by

$$\mathcal{L} = [\sigma_1 \boldsymbol{q}_1^T, \sigma_2 \boldsymbol{q}_2^T]^T \tag{13}$$

where $\boldsymbol{q}_i$ is the i-th column of $\boldsymbol{Q}$.

[9] Bartoli, Adrien , and P. Sturm . "Structure-from-motion using lines: Representation, triangulation, and bundle adjustment". Computer Vision and Image Understanding 100.3(2005):416-441.

Observation Model

- Line observation model

$$\varphi_{\mathcal{L}}\left(\boldsymbol{R}_{cg}, \boldsymbol{t}_{cg}, \mathcal{L}\right) = \begin{bmatrix} \boldsymbol{R}_{cg} & [\boldsymbol{t}_{cg}]_{\times}\boldsymbol{R}_{cg} \\ 0 & \boldsymbol{R}_{cg} \end{bmatrix} \cdot \begin{bmatrix} \tilde{\boldsymbol{u}} \\ \tilde{\boldsymbol{v}} \end{bmatrix} \tag{14}$$

where

$$\begin{bmatrix} \tilde{\boldsymbol{u}} \\ \tilde{\boldsymbol{v}} \end{bmatrix} = \frac{\mathcal{L}}{\|\boldsymbol{v}\|} \tag{15}$$

- $\boldsymbol{R}_{cg} \in \mathbb{SO}(3)$ and $\boldsymbol{t}_{cg} \in \mathbb{R}^3$ are the rotation matrix and the translation vector from the global coordinate frame to the camera coordinate frame, respectively.
- $[\boldsymbol{t}_{cg}]_{\times}$ is the skew symmetric matrix corresponding to $\boldsymbol{t}_{cg}$.

Generation of Line Shadows

- The origin of the camera frame w.r.t. the global frame is $\boldsymbol{O}_c = \boldsymbol{t}_{gc}$.
- The plane $\boldsymbol{\pi}_{\mathcal{L}}$ joining the line $\mathcal{L}$ and $\boldsymbol{O}_c$ is calculated by [10]

$$\boldsymbol{\pi}_{\mathcal{L}} \sim \boldsymbol{L}^* \cdot \tilde{\boldsymbol{O}}_c = \begin{bmatrix} [\boldsymbol{v}]_\times \boldsymbol{t}_{gc} + \boldsymbol{u} \\ -\boldsymbol{u}^T \boldsymbol{t}_{gc} \end{bmatrix} \tag{16}$$

where $\sim$ denotes the equality up to scale and $\tilde{\boldsymbol{O}}_c = [\boldsymbol{t}_{gc}^T, 1]^T$ is the homogeneous coordinates of the origin.

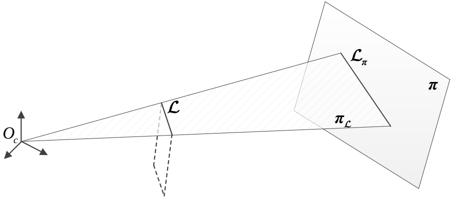

[10] R. Hartley and A. Zisserman, “Multiple View Geometry in Computer Vision”. Cambridge University Press, 2003, second Edition.

Generation of Line Shadows

- $\boldsymbol{L}^*$ is the dual Plücker matrix associated with $\boldsymbol{\mathcal{L}}$ which is computed by [11]

$$\boldsymbol{L}^* = \begin{bmatrix} [\boldsymbol{v}]_\times & \boldsymbol{u} \\ -\boldsymbol{u}^T & 0 \end{bmatrix} \tag{17}$$

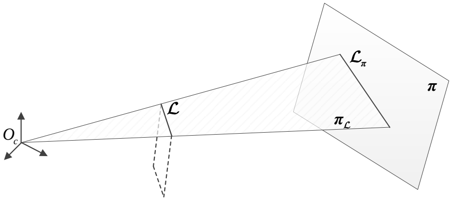

[11] R. Hartley and A. Zisserman, “Multiple View Geometry in Computer Vision”. Cambridge University Press, 2003, second Edition.

Generation of Line Shadows

- The occluded line on the plane $\boldsymbol{\pi}$ corresponding to the occluding line $\boldsymbol{\mathcal{L}}$ is denoted by $\boldsymbol{\mathcal{L}}_\pi$. The corresponding dual Plücker matrix $\boldsymbol{L}_\pi^*$ is calculated by

$$\boldsymbol{L}_\pi^* \sim \boldsymbol{\pi}\boldsymbol{\pi}_{\mathcal{L}}^T - \boldsymbol{\pi}_{\mathcal{L}}\boldsymbol{\pi}^T = \begin{bmatrix} [\boldsymbol{v}_\pi]_\times & \boldsymbol{u}_\pi \\ -\boldsymbol{u}_\pi^T & 0 \end{bmatrix} \quad (18)$$

$$\begin{aligned} \boldsymbol{u}_\pi &= -d([\boldsymbol{v}]_\times \boldsymbol{t}_{gc} + \boldsymbol{u}) - \boldsymbol{n}\boldsymbol{t}_{gc}^T\boldsymbol{u} \\ \boldsymbol{v}_\pi &= -[\boldsymbol{n}]_\times [\boldsymbol{v}]_\times \boldsymbol{t}_{gc} + [\boldsymbol{u}]_\times \boldsymbol{n} \end{aligned} \quad (19)$$

- The Plücker coordinates $\boldsymbol{\mathcal{L}}_\pi = [\boldsymbol{u}_\pi^T, \boldsymbol{v}_\pi^T]^T$.

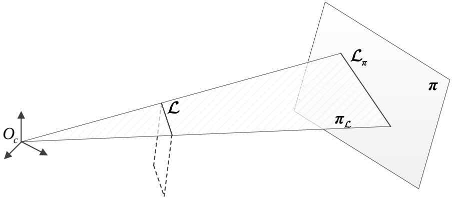

Observation Model

- Shadow observation model

$$\varphi_{\mathcal{L}\pi}(\boldsymbol{R}_{cg}, \boldsymbol{t}_{cg}, \boldsymbol{\mathcal{L}}, \boldsymbol{\pi}) = \begin{bmatrix} \boldsymbol{R}_{cg} & [\boldsymbol{t}_{cg}]_{\times}\boldsymbol{R}_{cg} \\ 0 & \boldsymbol{R}_{cg} \end{bmatrix} \cdot \begin{bmatrix} \tilde{\boldsymbol{u}}_{\pi} \\ \tilde{\boldsymbol{v}}_{\pi} \end{bmatrix} \tag{20}$$

where

$$\begin{bmatrix} \tilde{\boldsymbol{u}}_{\pi} \\ \tilde{\boldsymbol{v}}_{\pi} \end{bmatrix} = \frac{\boldsymbol{\mathcal{L}}_{\pi}}{\|\boldsymbol{v}_{\pi}\|} \tag{21}$$

Error Propagation from Lines and Planes to Shadows

- The covariance of the plane and line parameters are obtained by the pseudoinverse of the information matrices (computed in Section 4).

$$\boldsymbol{C}_{\pi} = \boldsymbol{\Omega}_{\pi}^{\dagger} = \begin{bmatrix} \boldsymbol{C}_{nn} & \boldsymbol{C}_{nd} \\ \boldsymbol{C}_{nd}^{T} & C_{dd} \end{bmatrix} \tag{22}$$

$$\boldsymbol{C}_{\mathcal{L}} = \boldsymbol{\Omega}_{\mathcal{L}}^{\dagger} = \begin{bmatrix} \boldsymbol{C}_{uu} & \boldsymbol{C}_{uv} \\ \boldsymbol{C}_{uv}^{T} & \boldsymbol{C}_{vv} \end{bmatrix} \tag{23}$$

- The covariance of the line shadow is computed by

$$\begin{aligned} \boldsymbol{C}_{\mathcal{L}\pi} &= \frac{\partial \boldsymbol{\mathcal{L}}_{\pi}}{\partial \boldsymbol{\pi}} \boldsymbol{C}_{\pi} \frac{\partial \boldsymbol{\mathcal{L}}_{\pi}}{\partial \boldsymbol{\pi}}^{T} + \frac{\partial \boldsymbol{\mathcal{L}}_{\pi}}{\partial \boldsymbol{\mathcal{L}}} \boldsymbol{C}_{\mathcal{L}} \frac{\partial \boldsymbol{\mathcal{L}}_{\pi}}{\partial \boldsymbol{\mathcal{L}}}^{T} \\ &= \begin{bmatrix} d^2 \boldsymbol{C}_{uu} + C_{dd} \boldsymbol{u}\boldsymbol{u}^T & d\boldsymbol{C}_{uu}[\boldsymbol{n}]_{\times}^{T} + \boldsymbol{u}\boldsymbol{C}_{nd}^{T}[\boldsymbol{u}]_{\times} \\ d[\boldsymbol{n}]_{\times}\boldsymbol{C}_{uu} + [\boldsymbol{u}]_{\times}\boldsymbol{C}_{nd}\boldsymbol{u}^T & [\boldsymbol{n}]_{\times}\boldsymbol{C}_{uu}[\boldsymbol{n}]_{\times}^{T} + [\boldsymbol{u}]_{\times}\boldsymbol{C}_{nn}[\boldsymbol{u}]_{\times}^{T} \end{bmatrix} \end{aligned} \tag{24}$$

$$\boldsymbol{\Omega}_{\mathcal{L}\pi} = \boldsymbol{C}_{\mathcal{L}\pi}^{\dagger} \tag{25}$$

Experiments - Fr3/cabinet

Scene

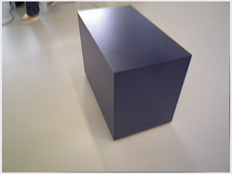

Relative Pose Error

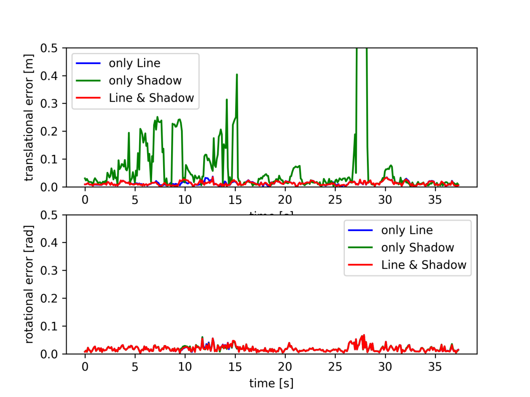

Experiments - Fr2/str_near

Scene

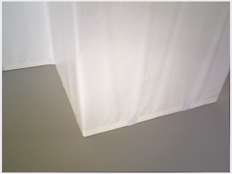

Relative Pose Error

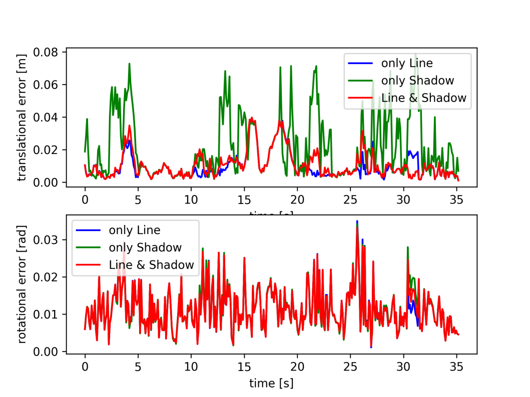

Experiments - Fr1/xyz

Scene

Relative Pose Error

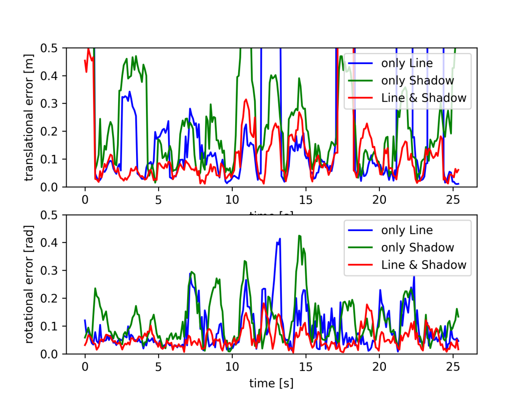

Experiments - Fr1/rpy[12]

Scene

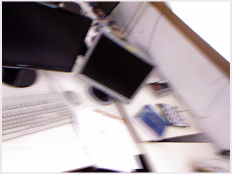

Relative Pose Error

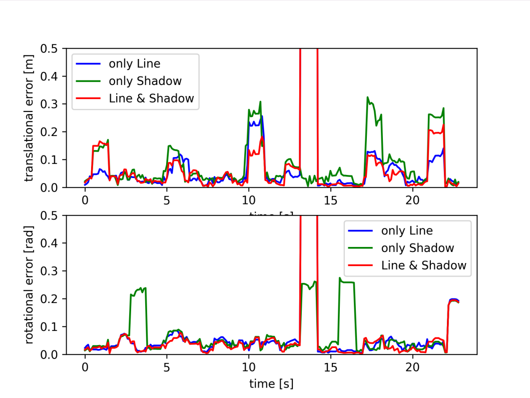

[12] groundtruth辅助数据关联

Experiments - Fr1/desk[13]

Scene

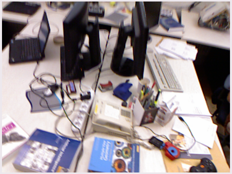

Relative Pose Error

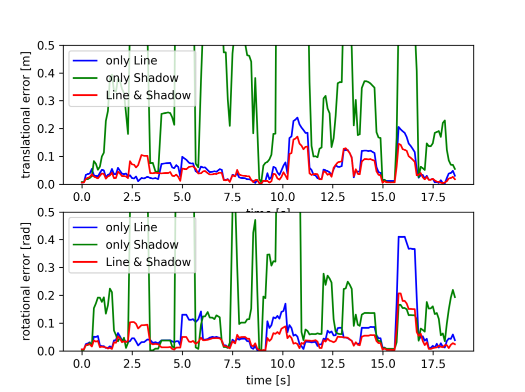

[13] groundtruth辅助数据关联

Experiments - Fr2/xyz[14]

Scene

Relative Pose Error

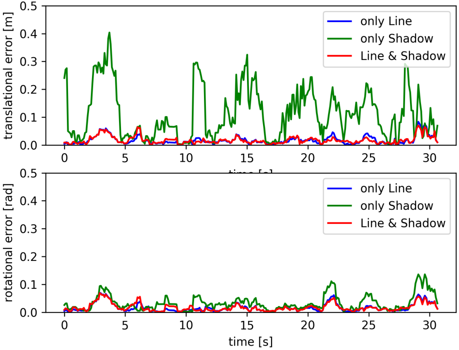

14 groundtruth辅助数据关联

Experiments - Fr2/rpy[15]

Scene

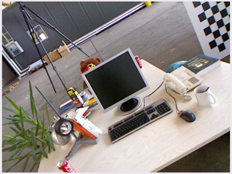

Relative Pose Error

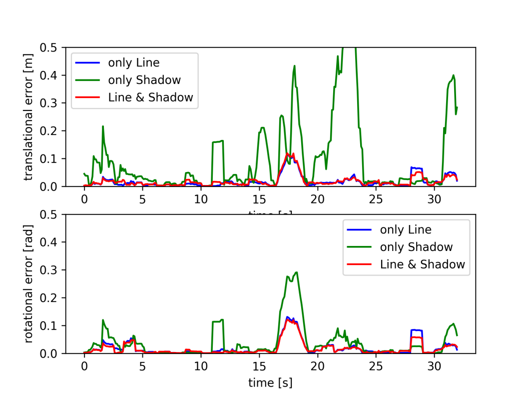

[15] groundtruth辅助数据关联

Experiments - Fr3/office[16]

Scene

Relative Pose Error

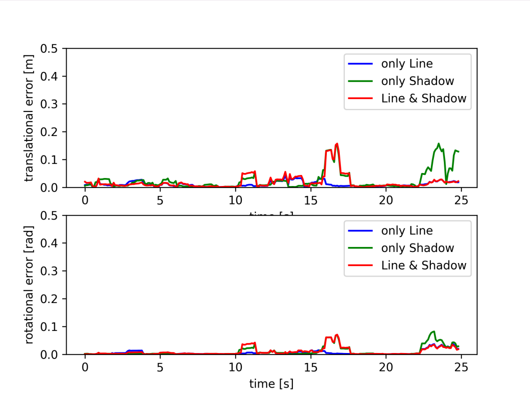

[16] groundtruth辅助数据关联

Constraint Analysis for Planes [17]

- The error vector for plane observation is

$$\boldsymbol{e}_\pi = \begin{bmatrix} {}^c\boldsymbol{n} \\ {}^c d \end{bmatrix} - \begin{bmatrix} \boldsymbol{R} & 0 \\ -\boldsymbol{t}^T\boldsymbol{R} & 1 \end{bmatrix} \begin{bmatrix} \boldsymbol{n} \\ d \end{bmatrix} \tag{26}$$

- The Jacobian matrix of $\boldsymbol{e}_\pi$ w.r.t. the minimal motion parameters $\boldsymbol{\xi} = [\boldsymbol{t}^T, \boldsymbol{\omega}^T]^T$ is calculated.

$$\frac{\partial \boldsymbol{e}_\pi}{\partial \boldsymbol{\xi}} = \begin{bmatrix} 0 & [\boldsymbol{Rn}]_\times \\ (\boldsymbol{Rn})^T & -\boldsymbol{t}^T[\boldsymbol{Rn}]_\times \end{bmatrix} \tag{27}$$

- The null space of $\frac{\partial \boldsymbol{e}_\pi}{\partial \boldsymbol{\xi}}$ is

$$\text{null}\left(\frac{\partial \boldsymbol{e}_\pi}{\partial \boldsymbol{\xi}}\right) = \begin{bmatrix} \mu_1\boldsymbol{t}_1 + \mu_2\boldsymbol{t}_2 \\ \mu_3(\boldsymbol{Rn}) \end{bmatrix} \tag{28}$$

with $\boldsymbol{t}_1$ and $\boldsymbol{t}_1$ are orthogonal vectors spanning the plane vertical to $\boldsymbol{Rn}$ and $\mu_1, \mu_2, \mu_3 \in \mathbb{R}$.

[17] Q. Sun, J. Yuan, X. Zhang and F. Duan, Plane-Edge-SLAM: Seamless Fusion of Planes and Edges for SLAM in Indoor Environments.

Constraint Analysis for Planes [18]

- For N_π plane observations

$$\sum_{j=1}^{N_\pi} \left(\frac{\partial \boldsymbol{e}_{\pi j}}{\partial \xi} d\boldsymbol{\xi} \right)^T \boldsymbol{\Omega}_{\pi j} \left(\frac{\partial \boldsymbol{e}_{\pi j}}{\partial \xi} d\boldsymbol{\xi} \right) = d\boldsymbol{\xi}^T \boldsymbol{\Psi}_\pi d\boldsymbol{\xi} \tag{29}$$

$$\boldsymbol{\Psi}_\pi = \sum_{j=1}^{N_\pi} \frac{\partial \boldsymbol{e}_{\pi j}}{\partial \xi}^T \boldsymbol{\Omega}_{\pi j} \frac{\partial \boldsymbol{e}_{\pi j}}{\partial \xi} \tag{30}$$

- Two degenerate cases:
    - 1-DoF unconstrained:
      $\exists \boldsymbol{e}$ such that $(\boldsymbol{R}\boldsymbol{n}_j)^T \boldsymbol{e} = 0, \ \forall j$
      unconstrained motion: $\boldsymbol{\xi} = [\mu \boldsymbol{e}^T, 0^T]^T$.
    - 3-DoF unconstrained:
      $\exists \boldsymbol{e}$ such that $(\boldsymbol{R}\boldsymbol{n}_j) \times \boldsymbol{e} = 0, \ \forall j$
      unconstrained motion: $\boldsymbol{\xi} = [(\mu_1 \boldsymbol{t}_1 + \mu_2 \boldsymbol{t}_2)^T, \mu_3 \boldsymbol{e}^T]^T$.

[18] Q. Sun, J. Yuan, X. Zhang and F. Duan, Plane-Edge-SLAM: Seamless Fusion of Planes and Edges for SLAM in Indoor Environments.

Constraint Analysis for Line

- The error vector for line observation is

$$\boldsymbol{e}_{\mathcal{L}} = \begin{bmatrix} {}^{c}\tilde{\boldsymbol{u}} \\ {}^{c}\tilde{\boldsymbol{v}} \end{bmatrix} - \begin{bmatrix} \boldsymbol{R} & [\boldsymbol{t}]_{\times}\boldsymbol{R} \\ 0 & \boldsymbol{R} \end{bmatrix} \begin{bmatrix} \tilde{\boldsymbol{u}} \\ \tilde{\boldsymbol{v}} \end{bmatrix} \tag{31}$$

- The Jacobian matrix of $\boldsymbol{e}_{\mathcal{L}}$ w.r.t. $\boldsymbol{\xi}$ is

$$\frac{\partial \boldsymbol{e}_{\mathcal{L}}}{\partial \boldsymbol{\xi}} = \begin{bmatrix} [\boldsymbol{R}\tilde{\boldsymbol{v}}]_{\times} & [\boldsymbol{R}\tilde{\boldsymbol{u}}]_{\times} + [\boldsymbol{t}]_{\times}[\boldsymbol{R}\tilde{\boldsymbol{v}}]_{\times} \\ 0 & [\boldsymbol{R}\tilde{\boldsymbol{v}}]_{\times} \end{bmatrix} \tag{32}$$

- The null space of $\frac{\partial \boldsymbol{e}_{\mathcal{L}}}{\partial \boldsymbol{\xi}}$ is

$$\operatorname{null}\left(\frac{\partial \boldsymbol{e}_{\mathcal{L}}}{\partial \boldsymbol{\xi}}\right) = \mu_1 \begin{bmatrix} \boldsymbol{R}\tilde{\boldsymbol{u}} \\ \boldsymbol{R}\tilde{\boldsymbol{v}} \end{bmatrix} + \mu_2 \begin{bmatrix} \boldsymbol{R}\tilde{\boldsymbol{v}} \\ 0 \end{bmatrix} \tag{33}$$

with $\mu_1, \mu_2 \in \mathbb{R}$.

Constraint Analysis for Lines

- For $N_{\mathcal{L}}$ line observations

$$\sum_{k=1}^{N_{\mathcal{L}}} \left(\frac{\partial \boldsymbol{e}_{\mathcal{L}k}}{\partial \xi} d\boldsymbol{\xi} \right)^T \boldsymbol{\Omega}_{\mathcal{L}k} \left(\frac{\partial \boldsymbol{e}_{\mathcal{L}k}}{\partial \xi} d\boldsymbol{\xi} \right) = d\boldsymbol{\xi}^T \boldsymbol{\Psi}_{\mathcal{L}} d\boldsymbol{\xi} \tag{34}$$

$$\boldsymbol{\Psi}_{\mathcal{L}} = \sum_{k=1}^{N_{\mathcal{L}}} \frac{\partial \boldsymbol{e}_{\mathcal{L}k}}{\partial \xi}^T \boldsymbol{\Omega}_{\pi j} \frac{\partial \boldsymbol{e}_{\mathcal{L}k}}{\partial \xi} \tag{35}$$

- Two degenerate cases:
  - 1-DoF unconstrained:
    $\exists \boldsymbol{e}$ such that $(\boldsymbol{R}\tilde{\boldsymbol{v}}_k) \times \boldsymbol{e} = 0, \ \forall k$
    unconstrained motion: $\boldsymbol{\xi} = [\mu \boldsymbol{e}^T, 0]^T$.
  - 2-DoF unconstrained:
    There is only one line.
    unconstrained motion: $\boldsymbol{\xi} = \mu_1 [\tilde{\boldsymbol{u}}^T, \tilde{\boldsymbol{v}}^T]^T + \mu_2 [\tilde{\boldsymbol{v}}^T, 0^T]^T$.

Degenerate Cases for Planes and Lines

- Degenerate cases for planes and lines:
  - 1-DoF unconstrained:
    $\exists \boldsymbol{e}$ such that $(\boldsymbol{R}\boldsymbol{n}_j)^T\boldsymbol{e} = 0,\ \forall j$ and $(\boldsymbol{R}\tilde{\boldsymbol{v}}_k) \times \boldsymbol{e} = 0,\ \forall k$.
    unconstrained motion: $\boldsymbol{\xi} = [\mu\boldsymbol{e}^T, 0]^T$.
  - 1-DoF unconstrained:
    There is only one line and $\exists \boldsymbol{e}$ such that $(\boldsymbol{R}\boldsymbol{n}_j) \times \boldsymbol{e} = 0,\ \forall j$.
    unconstrained motion: $\boldsymbol{\xi} = \mu[\tilde{\boldsymbol{u}}^T, \tilde{\boldsymbol{v}}^T]^T$.

Maximum Likelihood for Plane Fitting